# Isotopic Preservation of Himalayan/Tibetan Uplift, Denudation, and Climatic Histories of Two Molasse Deposits[1]

*T. Mark Harrison, Peter Copeland[2], Stuart A. Hall[2], Jay Quade[3], Scott Burner, T. P. Ojha[4], and W. S. F. Kidd[5]*

*Dept. of Earth and Space Sciences, University of California, Los Angeles, CA 90024 USA*

## ABSTRACT

Two distinctive molasse deposits within the Indo-Asian collision zone have been investigated to help understand the post-Oligocene evolution of the Himalaya and southern Tibetan plateau. The Siwalik Group (predominantly fluvial sandstones and siltstones), is widespread throughout the foothills of the Himalaya from Pakistan to eastern India. Paleomagnetic analysis of a measured section in the Bakiya Khola, southeastern Nepal, constrains depositional ages ($t_{dep}$) to between 10.8 and 4.9 Ma. The average accumulation rate during this interval was 0.4–0.5 mm/yr. $^{40}Ar/^{39}Ar$ dating of 126 detrital K-feldspars from nine horizons in the Bakiya Khola section ($t_{dep}$ = 8.25 to ~2.2 Ma) provide snapshots in time of the cooling ages exposed at the earth's surface in this drainage basin. The minimum age in the spectra from seven of the nine horizons averages only 3 m.y. older than $t_{dep}$, indicating exceptionally rapid unroofing in the Himalaya throughout that interval. Half of the grains from these nine sections yield minimum ages between 5 and 21 Ma. This latter age corresponds to the onset of a widespread unroofing event throughout the Himalaya and southern Tibet. Carbonates in paleosols exposed along Bakiya Khola yield carbon isotopic values averaging $-10.5 \pm 0.8$‰ $\delta^{13}C_{PDB}$ between 11 and 7.0 Ma, and about 0‰ $\delta^{13}C$ between 7.4 Ma to the top of the section at about 2 Ma. This shift, previously recognized in Siwalik Group sediments in Pakistan, is interpreted to result from a change from dominantly $C_3$ plants (i.e., trees) to dominantly $C_4$ plants (i.e., grasses). The first appearance of $C_4$ grasses favored by a warm growing season marks a significant ecological shift that may be related to intensification of the Asian Monsoon brought about by uplift of the Tibetan Plateau. In south-central Tibet, the Kailas conglomerate developed a thickness of over 3 km due to uplift and erosion of the Gangdese belt. Age assessment of this unit has been problematic (Late Eocene to Miocene?). $^{40}Ar/^{39}Ar$ K-feldspar results from a cobble from the Kailas conglomerate, presumed to be from the Gangdese volcanic suite, yields an age spectrum characterized by relatively slow cooling (5°C/Ma) between 27–19 Ma followed by very rapid cooling (100°C/Ma) between 19–18 Ma. The feldspar microstructure indicates that it has been heated to >400°C subsequent to eruption. This thermal history is consistent with deep burial in the volcanic pile subsequent to extrusion followed by rapid unroofing beginning at 20 to 19 Ma. These results suggest an Early Miocene upper limit for the depositional age of the Kailas conglomerate, and extends the evidence for a substantially enhanced unroofing at this time in the Gangdese-Himalaya system.

## Introduction

The evolutionary record of a mountain belt preserved in the form of sedimentary rocks has been pivotal in developing our understanding of orogeny. The utility of sediments in establishing a tectonic context for basin development is evidenced by continuing refinements of techniques to decipher this record (e.g., Dickinson 1974; Ingersoll 1988). These approaches generally emphasize characteristic changes in clastic mineral abundances as an indicator of the dominant tectonic style. However, individual detrital grains can retain an even more informative record of provenance, including information regarding the age of the source and its cooling history. With the advent of high-sensitivity isotopic techniques, it is now possible

[1] Manuscript received June 15, 1992; accepted December 1, 1992.

[2] Department of Geosciences, University of Houston, Houston, TX 77204-5503 USA.

[3] Department of Geological Sciences, University of Arizona, Tucson, AZ 85721 USA.

[4] Petroleum Exploration Project, Dept. of Mines and Geology, Geological Survey of Nepal, Lainchaur, Kathmandu, Nepal.

[5] Department of Geological Sciences, SUNY at Albany, Albany, NY 12222 USA.

[The Journal of Geology, 1993, volume 101, p. 157–175]  0022-1376/93/0102-006$1.00

to interrogate discrete grains, even in relatively fine-grained sedimentary rocks, to reveal isotopic variations with high precision (e.g., Froude et al. 1983; Cerveny et al. 1988; Copeland and Harrison 1990).

$^{40}Ar/^{39}Ar$ mineral ages in orogenic terranes generally reflect cooling due to unroofing. Thus, a grain exposed at the earth's surface may retain, in the form of isotopic gradients, cooling information reflecting denudation processes that in turn may be related to surface uplift rates. For example, material from basement outcrops throughout the Indo-Asian collision zone yields thermochronological results to help constrain models of tectonic evolution (Harrison et al. 1992*a*). However, this approach is limited by the fact that only a narrow depth range within the lithosphere has a temperature distribution appropriate to recording $^{40}Ar/^{39}Ar$ thermochronological information. This means that, in general, very few rocks presently exposed will contain information about denudation/uplift during a specific period. It would greatly enhance our understanding of the collision zone if we could travel back in time to sample basement material then exposed at the earth's surface. Fortunately, each stratum of sedimentary rock is, in effect, a time-machine containing a population of grains that preserves the thermal histories represented by basement rocks exposed just prior to deposition.

Copeland and Harrison (1990) applied this approach on samples from drill cores in the Bengal Fan to learn whether portions of the Indo-Asian collision zone were rapidly unroofing throughout the Neogene. They performed low-resolution $^{40}Ar/^{39}Ar$ step-heating experiments on detrital K-feldspar grains from depth intervals corresponding to ages 18–2 Ma. Surprisingly, they found cooling ages within analytical uncertainty of the stratigraphic age in every depth interval investigated, suggesting very high rates of unroofing in some places within the collision zone.

To utilize $^{40}Ar/^{39}Ar$ results from clastic grains to reveal past unroofing events, the "time machine" must first be calibrated. In the case of the marine sediments of the Bengal Fan, this was provided by chronostratigraphic interpretation of the paleontological record (e.g., Gartner 1990; Cochran 1990). However, sediments closer to the crustal thickening should contain an even clearer picture of the evolution of the collision zone by avoiding detritus added from sources outside the orogen.

The Himalaya and Tibetan Plateau are the result of the northward convergence of India into Asia over the past 50 m.y. Despite this clear relationship, details of the timing and mechanisms responsible for the present topography remain controversial. Understanding the relative importance of crustal thickening (e.g., Dewey and Burke 1973) and lateral extrusion of crustal blocks along strike-slip faults (e.g., Tapponnier et al. 1986) in accommodating this shortening is fundamental to an understanding of the evolution of Tibet and the Himalaya. Since each evolutionary model makes different predictions regarding the timing of uplift and consequent denudation (Harrison et al. 1992*a*), a possible key to distinguish when these various mechanisms operated within the collision zone may be locked within sedimentary deposits.

Tremendous amounts of sediment have accumulated in molasse basins both in front of the Himalaya (the Siwalik Group, which varies between 5 and 8 km thickness) and in the Gangdese plutonic belt of southern Tibet. Unfortunately, these terrestrial sediments lack fossil assemblages that would permit precise age assignment and thus require an alternate approach. Johnson et al. (1982, 1985) sidestepped this limitation by using magnetostratigraphy to calibrate age relationships in Siwalik Group sediments in northern Pakistan.

In this paper, we report preliminary investigations of two contrasting sites of molasse deposition within the Indo-Asian orogen—the Siwalik Group exposed in the Bakiya Khola, southeastern Nepal (figures 1, 2), and the Kailas conglomerate in south-

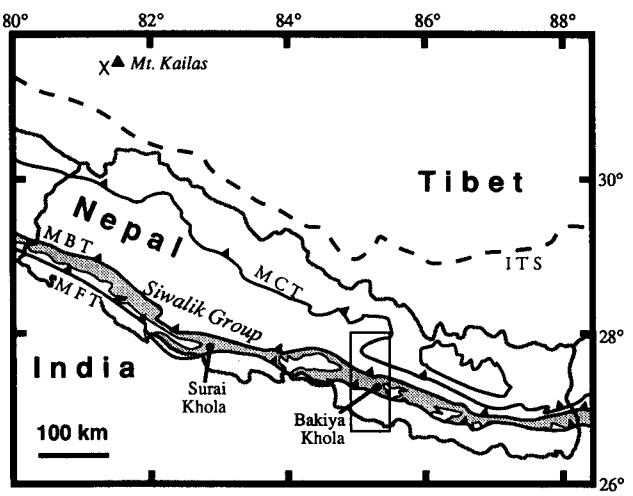


**Figure 1.** Geologic sketch map of Nepal and surrounding areas showing distribution of the Siwalik Group (shaded) and major tectonic structures. ITS = Indus Tsangpo Suture; MCT = Main Central Thrust; MBT = Main Boundary Thrust; MFT = Main Frontal Thrust. Box shows location of figure 2. "X" marks the location of sample from Kailas conglomerate.

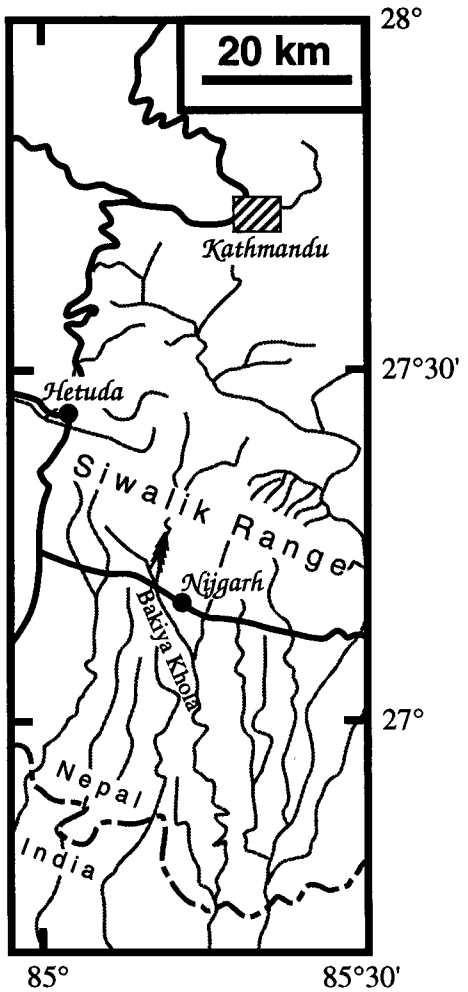


**Figure 2.** Map showing location of the Bakiya Khola section in southeastern Nepal and major highways and principal drainages. Chevron pattern shows location of the Bakiya measured section; heavy lines are roads; stippled lines are rivers; dashed line is the international border.

central Tibet (figure 1). These studies demonstrate varied methods for wresting uplift/denudation histories from clastic sedimentary rocks. Our approach for the Siwalik Group (Bakiya Khola) was first to obtain depositional ages by magnetostratigraphic analysis of the siltstones and finer-grained sandstones. We then used $^{40}Ar/^{39}Ar$ analyses of K-feldspar from coarser sandstones to establish unroofing patterns, and stable isotope measurements of soil carbonate to determine paleoclimatic variations through time. Near Mt. Kailas, we used $^{40}Ar/^{39}Ar$ measurements of K-feldspar separated from a single meta-rhyolite cobble within a thick conglomerate section to infer a thermal history for the protolith and the approximate depositional age of the clast.

## Site Descriptions

The Kailas conglomerate was deposited on the southern slope of an (inactive) Andean-type plutonic belt, accumulating a thickness of >3 km (Gansser 1964). Clasts are largely volcanic and derived from the Gangdese magmatic complex directly to the north. Isotopic investigations of a variety of plutonic and volcanic rocks from this suite (e.g., diorite, granodiorite, leucogranite, rhyolite), both in outcrop and pebbles from the conglomerate, indicate that eruption and emplacement occurred in the interval 41 to 37 Ma (Honegger et al. 1982).

The Bakiya Khola section, southeastern Nepal (figures 1, 2), was chosen for intensive investigation for several reasons: the continuous exposure of much of the section, which is remarkably undeformed relative to other well-characterized Siwalik sections in Nepal (e.g., Corvinus 1988), its location in eastern Nepal, which permits examination of a geographic variation in the onset of the carbon isotope shift (Quade et al. 1989), and because the region of best characterized basement $^{40}Ar/^{39}Ar$ cooling ages lies in the direction (NW) of the sediment source (Copeland et al. 1990*a*, 1991).

A 2600 m section of Siwalik Group sediments (Gansser 1964) was measured in the Bakiya Khola (figure 3). These generally W to NW striking beds dip N between 30–60°. The lower 2100 m of section is essentially continuous and relatively undeformed compared to other sections of the Nepalese Siwaliks. A large bend in the Bakiya Khola offsets the upper 500 m of measured section, but this portion could be correlated because of the good exposure and relatively simple structure. Beyond the measured section, an additional ~1000 m of intermittently exposed strata was examined in a reconnaissance fashion and sampled for paleosols (not in figure 8) and $^{40}Ar/^{39}Ar$ analyses. A further 500 m has not yet been examined, and additional strata may be present. The lithologies in this section are dominantly siltstones and sandstones. In the lower part of the section the sandstones vary in thickness from 1 to 5 m, with intervening finer-grained strata up to 2 m thick. Above 1000 m the sandy layers reach thicknesses of up to 40 m with thin (<1 m) interbedded siltstones. The composition of the sandstones is arkosic with abundant coarse micas (mostly muscovite). The size of sand grains is fine to medium below 1000 m, increasing to medium to coarse in the upper parts of the section with rare

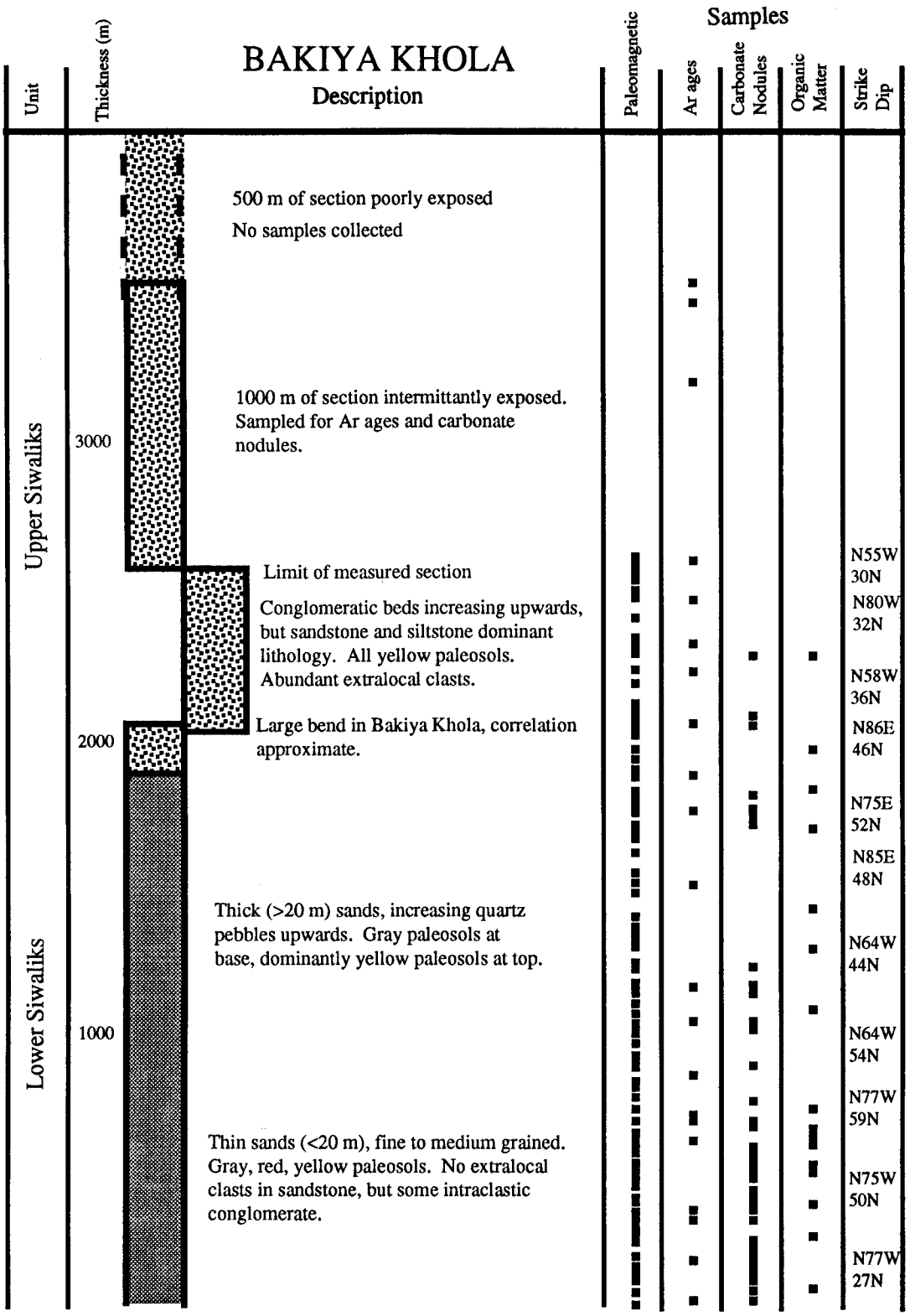


**Figure 3.** Simplified stratigraphic section of Siwalik Group sediments in the Bakiya Khola, southern Nepal, showing locations of samples taken for the various analyses.

rock fragments up to 4 cm across; sorting decreases with stratigraphic height. These characteristics suggest that the section of the Siwalik Group exposed at Bakiya Khola is best characterized as a part of the Lower Siwaliks (LS) or the lower part of the Middle Siwaliks (MS1).

## Analytical Details

***Paleomagnetism.*** Samples were taken from siltstones and fine-grained sandstones. Where possible, horizons with well-preserved bedding were collected, although bioturbated horizons such as paleosols were also occasionally sampled. On average, we took one sample every 30 m as lithology permitted. This sampling density could not be maintained in the sandstone-rich middle of the section. A smooth surface was first formed on a specimen in situ with a coarse rasp. The sample was then oriented using a Brunton compass, marked, and subsequently extracted using a hammer and wedge. Three samples from each paleomagnetic site were obtained. These hand specimen-sized samples were sawed into cubes (typically 5 cm on edge) and cored to make 2.5 cm diameter cylinders of 1–2.5 cm length. Some samples were lost during drilling due to high clay content. The natural remanent magnetism of these specimens was measured using a two-component cryogenic magnetometer housed in a shielded room at the University of Houston following the procedures of Beaubouef et al. (1990). To isolate stable components of remanence, samples (including several pairs of samples from the same horizon) were subjected to thermal demagnetization. Samples were heated to 50°C, cooled in a low field environment ($<5nT$) and the remaining remanence determined. The samples were then heated to 500°C in 50°C increments and their remanence measured after each heating step.

***Carbon and Oxygen Isotopes.*** Carbon and oxygen isotopes were measured on 34 carbonate nodules recovered from paleosol horizons and four organic samples in Siwalik Group sediments exposed in the Bakiya Khola. The carbonate nodules were first crushed to $-40 + 100$ mesh and bleached in a 5.25% solution of NaClO for one hour at 40–50°C, and then overnight at room temperature. The bleach was removed from the samples by centrifuging in 2D water until the pH of the distilled water was unchanged by the interaction. Samples were then frozen in a freeze dryer to sublime any remaining water. About 30 mg of each sample was weighed into a reaction vessel and the $CO_2$ extracted by conventional methods (McCrea 1950). Isotopic measurements of carbon and oxygen were performed at UCLA and the Australian National University using MAT 251/252 mass spectrometers. Carbon and oxygen isotopic data are given in table 1.

***$^{40}Ar/^{39}Ar$.*** A single 11 × 7 × 3 cm cobble from the Kailas conglomerate was obtained for this study. Although its appearance in hand specimen is of a felsic volcanic or hypabyssal rock, this rock has the character of a recrystallized plutonic rock in thin section. Millimeter-scale alkali feldspar phenocrysts observed in hand specimen are perthitic and in contact with peripheral albite blebs that appear to be an early phase of exsolution (figure 4). The perthite is about 75% K-feldspar. The close association of the albite blebs and large perthites, as well as their complete separation, suggests fluid-assisted coarsening, perhaps in a hydrothermal system immediately following intrusion/emplacement. Electron microprobe analysis reveals the K-feldspar to be $Or_{97}$ and the albite blebs to be $Or_3$. This unusual relationship may reflect a two-stage thermal history that provides a useful constraint on the denudation and burial history.

Fresh, hand-sized samples of incompletely consolidated coarse sandstones from the Bakiya Khola were obtained during fieldwork in April, 1991. These samples were gently crushed, eluted in water, and sized to between 0.15 and 2 mm. K-feldspar separates were obtained using heavy liquid and magnetic separatory techniques. Splits of K-feldspar were wrapped in Sn foil and sealed in 6 mm ID evacuated quartz glass vials together with Fish Canyon sanidine (FC-3) flux monitors and irradiated in the H-5 position of the Ford Reactor, University of Michigan (see Harrison et al. 1991*a* for irradiation details). Aliquants of monitor crystals were individually fused and analyzed for their argon isotopic composition. The pooled $^{40}Ar/^{39}Ar_K$ results yielded a J factor for the Kailas K-feldspar of 0.01021, assuming an age of 27.8 Ma for FC-3 (Miller et al. 1985). Correction factors used for interfering neutron reactions were $(^{40}Ar/^{39}Ar)_K$ = 0.021 (±3%), $(^{39}Ar/^{37}Ar)_{Ca} = 5.06 \times 10^{-4}$ and $(^{36}Ar/^{37}Ar)_{Ca} = 2.3 = 10^{-4}$.

A 10 mg aliquant of the Kailas K-feldspar was step-heated in a Ta crucible within a double-vacuum furnace (see McDougall and Harrison 1988) in the cyclic fashion described by Harrison et al. (1991*a*) to enhance retrieval of kinetic information. Because of the difficulty manipulating the very small Siwalik K-feldspars in the resistance furnace, argon was released from these crystals by heating with a 5 W Ar-ion laser. However, analysis of alkali feldspars by this method is restricted by

**Table 1.** Stable Isotope Data for Pedogenic Carbonate and Organic Material from Bakiya Khola

| Lab | Sample ID (Bak-) | strat. height (km) | (Ma) | sample mass (mg) | $CO_2$ (μmol) | $\delta^{13}C$ | 1σ | $\delta^{18}O$ |
|---|---|---|---|---|---|---|---|---|
| UCLA | 4 | .012 | 10.95 | 50.00 | 260 | −9.99 | | −9.15 |
| UCLA | 10 | .045 | 10.80 | 30.10 | 179 | −10.13 | | −10.04 |
| ANU | 11 | .056 | 10.72 | 16.12 | 61 | −10.63 | .02 | −9.57 |
| ANU | 17 | .105 | 10.60 | 14.28 | 87 | −9.08 | .09 | −8.55 |
| UCLA | 17 | .105 | 10.60 | 30.00 | 136 | −9.48 | | −8.75 |
| UCLA | 18 | .124 | 10.48 | 35.10 | 200 | −10.51 | | −8.52 |
| UCLA | 23 | .149 | 10.35 | | | −8.59 | | −8.19 |
| UCLA | 28 | .194 | 10.25 | 30.00 | 121 | −10.48 | | −9.78 |
| UCLA | 43 | .334 | 9.88 | | | −10.88 | | −7.74 |
| ANU | 47 | .367 | 9.78 | | | −10.80 | | −7.70 |
| UCLA | 47 | .367 | 9.78 | 30.20 | 167 | −10.82 | | −8.01 |
| UCLA | 52 | .407 | 9.71 | | | −10.13 | | −9.91 |
| UCLA | 53-1 | .415 | 9.67 | | | −9.19 | | −8.69 |
| UCLA | 53-2 | .415 | 9.67 | | | −9.56 | | −9.54 |
| UCLA | 53-3 | .415 | 9.67 | | | −9.25 | | −8.78 |
| ANU | 57 | .438 | 9.63 | 14.90 | 93 | −10.49 | .02 | −7.50 |
| UCLA | 57 | .438 | 9.63 | 30.00 | 187 | −10.73 | | −8.23 |
| UCLA | 62 | .492 | 9.51 | | | −11.43 | | −10.09 |
| ANU | 76 | .648 | 9.14 | 12.20 | 53 | −9.98 | .02 | −8.49 |
| UCLA | 76 | .648 | 9.14 | 30.00 | 149 | −10.49 | | −8.42 |
| UCLA | 77 | .655 | 9.12 | 30.00 | 176 | −10.84 | | −8.52 |
| ANU | 90 | .759 | 8.89 | 14.70 | 106 | −9.36 | .01 | −8.60 |
| ANU | 98 | .952 | 8.44 | 13.38 | 73 | −9.67 | .02 | −10.40 |
| UCLA | 98 | .952 | 8.44 | 35.20 | 184 | −10.11 | | −10.03 |
| ANU | 104 | 1.033 | 8.29 | 14.70 | 66 | −11.33 | .02 | −6.70 |
| UCLA | 104A | 1.033 | 8.29 | 44.60 | 210 | −11.19 | | −7.44 |
| UCLA | 104B | 1.033 | 8.29 | 29.40 | 140 | −10.98 | | −7.82 |
| UCLA | 106 | 1.045 | 8.26 | | | −11.66 | | −7.47 |
| ANU | 115 | 1.199 | 7.90 | 14.53 | 78 | −11.28 | .01 | −10.30 |
| UCLA | 115 | 1.199 | 7.90 | 30.50 | 175 | −11.28 | | −10.25 |
| ANU | 117 | 1.229 | 7.82 | 14.80 | 87 | −11.46 | .03 | −7.10 |
| UCLA | 117 | 1.229 | 7.82 | | | −11.66 | | −8.64 |
| UCLA | 133 | 1.443 | 7.44 | | | −24.07 | | |
| ANU | 144 | 1.742 | 6.97 | 13.66 | 65 | −11.08 | .03 | −9.96 |
| UCLA | 144 | 1.742 | 6.97 | 30.50 | 80 | −11.31 | | −9.93 |
| ANU | 145 | 1.743 | 6.96 | 14.00 | 78 | −10.65 | .03 | −7.40 |
| ANU | 145 | 1.743 | 6.96 | 14.58 | 69 | −10.47 | .01 | −7.40 |
| ANU | 146 | 1.779 | 6.89 | 15.20 | 42 | −0.79 | .22 | −5.70 |
| UCLA | 146 | 1.779 | 6.89 | 29.70 | 61 | −1.50 | | −7.69 |
| ANU | 152 | 1.779 | 6.89 | 13.97 | 52 | −7.43 | .01 | −8.40 |
| UCLA | 152A | 1.875 | 6.80 | 29.40 | 135 | −10.27 | | −8.79 |
| UCLA | 152B | 1.875 | 6.80 | 30.20 | 116 | −7.29 | | −1.32 |
| UCLA | 156 | 1.893 | 6.77 | | | −24.73 | | |
| ANU | 168 | 2.054 | 6.11 | 15.43 | 77 | −10.64 | .02 | −7.60 |
| UCLA | 168 | 2.054 | 6.11 | 31.00 | 122 | −9.61 | | −8.66 |
| ANU | 179A | 2.364 | 5.32 | 145.02 | 29 | −13.54 | .02 | |
| ANU | 120 | 3.200 | 3.40 | 13.71 | 50 | −15.80 | .01 | −6.50 |
| UCLA | 120 | 3.200 | 3.40 | | | −15.82 | | |
| UCLA | 121-1 | 3.220 | 3.40 | | | 1.82 | | −6.00 |
| UCLA | 121-2 | 3.220 | 3.40 | | | 1.53 | | −6.08 |
| UCLA | 121-3 | 3.220 | 3.40 | | | 1.64 | | −6.17 |

Note. All samples are carbonates except for BAK133, BAK156, BAK179A, and BAK120, which are organic.

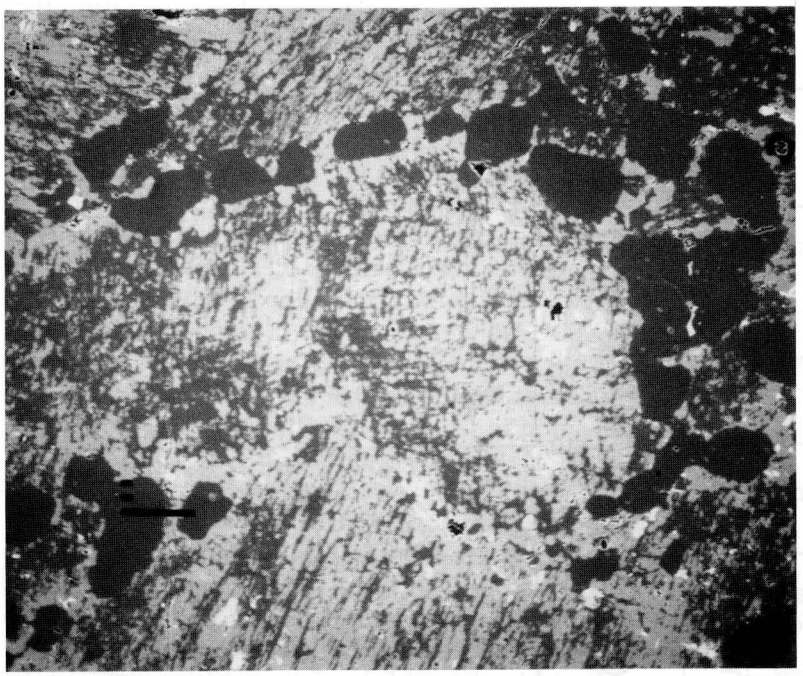

**Figure 4.** Backscattered electron micrograph of alkali feldspar in cobble from the Kailas conglomerate; long dimension of image is 1 mm. Two scales of exsolution are apparent. Blebs of albite form near the rims of mm-sized alkali feldspars that contain μm-scale perthite development, indicating a bulk composition of about $Or_{75}$.

their generally poor coupling with visible laser light (Copeland et al. 1990*b*). K-feldspars of ~200 μm diameter can generally be made to glow orange upon application of about 100–500 mW of laser power. Despite continued application of the light, the glow usually fades within seconds as internal features that couple the light are annealed. It is relatively easy during laboratory heating to modify a feldspar to prevent fusion of the crystal with 6 W of laser power. Thus it is a priori impossible to dictate a heating schedule that will release the gas in a systematic fashion. This explains the low resolution of our $^{40}Ar/^{39}Ar$ step-heating results. Our objective is to release the argon in at least two or three steps to obtain the minimum age in the spectrum that we associate with a closure temperature ($T_c$) of 150–200°C (see Copeland et al. 1990*b*).

Argon blanks over the course of these analyses averaged $2 \times 10^{-16}$ mol $^{40}Ar$ in an atmospheric ratio for both laser and resistance furnace systems. $^{40}Ar/^{39}Ar$ isotopic measurements were made using a VG 1200S (Baur 1980) mass spectrometer, operated in the electron multiplier mode, and a VG 3600 (Nier-type source) mass spectrometer, operated in Daly detector mode. A correction for mass discrimination of ~0.13%/amu was made to the isotope ratios based on analysis of atmospheric argon. Overall sensitivity for the spectrometer during these analyses was between $1–2 \times 10^{-17}$ mol Ar/mV. Further details of the experimental procedures are given in Harrison et al. (1991*a*), and details of peak height measurements and calculation of associated uncertainties are given in McDougall and Harrison (1988). Tabulated results of the argon isotopic analyses, uncorrected for neutron-produced interferences, with ages calculated using conventional decay constants and isotope abundances, are available from the authors on request.

***Rb-Sr and Sm-Nd.*** Isotopic and elemental analysis of a whole-rock split of the clast from the Kailas conglomerate following the procedures of Nelson and Davidson et al. (1992) were performed.

## Results

***Kailas.*** Because virtually all tectonophysical processes involve heat flow discontinuities, cooling-related isotopic variations preserved within minerals can be used as evidence of past tectonic activity. By imaging the internal distribution of $^{40}Ar$ produced from the in situ decay of $^{40}K$, the $^{40}Ar/^{39}Ar$ step-heating method provides the basis to retrieve thermal history information from a slowly cooled sample (McDougall and Harrison 1988). To obtain the thermal history content of an age spectrum, we use an extension of the single diffusion domain/activation energy closure theory (Dodson 1973) that applies to minerals with a discrete distribution of domain sizes or activation energies (Lovera et al. 1989, 1991, 1993; Harrison et al. 1991*a*). Arrhenius plots and age spectra derived from the thermal degassing of such samples

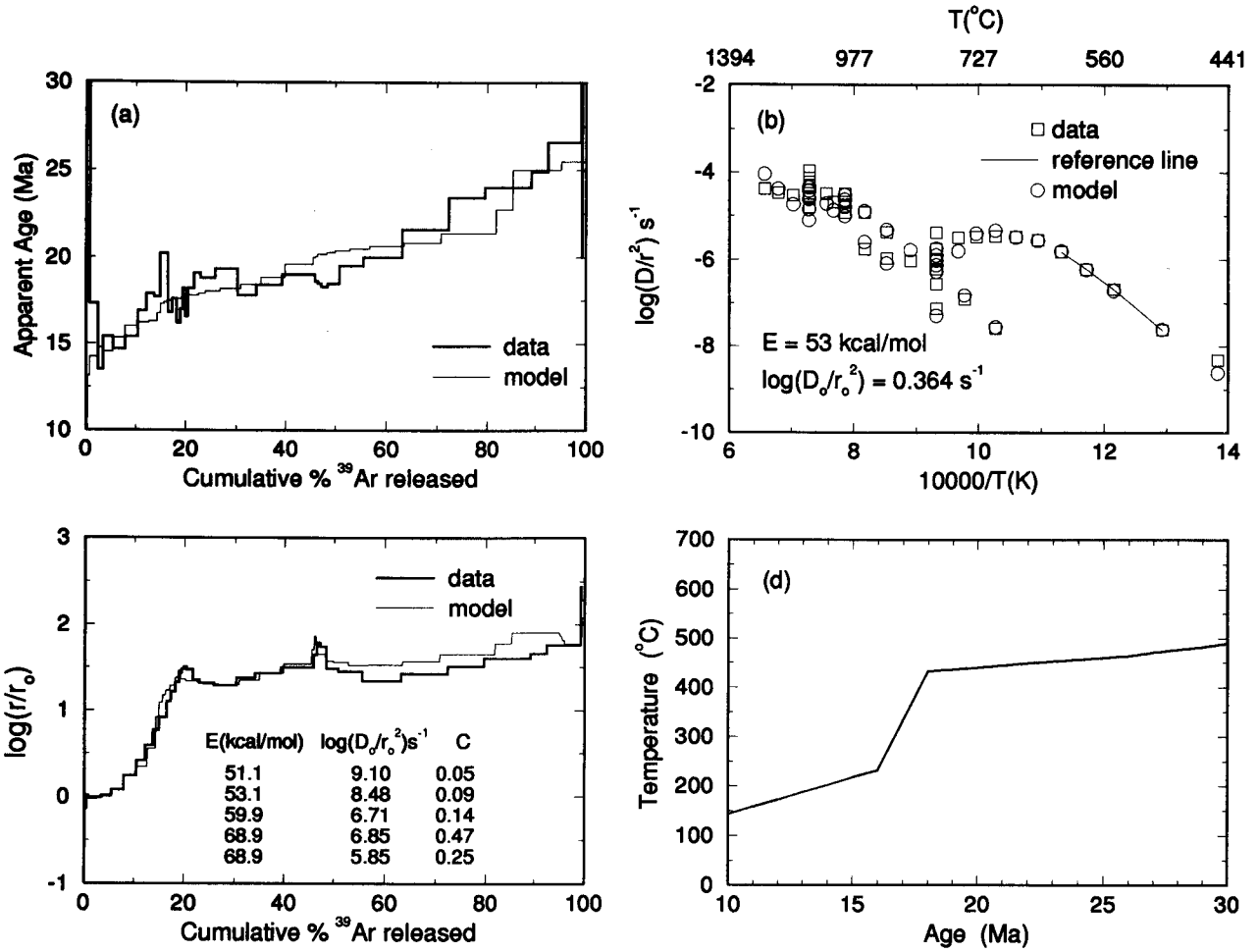


**Figure 5.** (*a*) $^{40}Ar/^{39}Ar$ age spectrum, (*b*) Arrhenius plot, (*c*) log $(r/r_O)$ plot, and (*d*) thermal history for a K-feldspar separated from a cobble of Kailas conglomerate. These results indicate rapid cooling at about 19 Ma.

are a mixture of those characterizing the individual diffusion domains. The diffusion parameters (activation energy, $E$, and frequency factor, $D_0/\rho^2$) for each discrete domain are obtained by iterating between fits to the Arrhenius plot and age spectrum. Once the diffusion parameters have been acquired, the thermal history is obtained by repeated forward modeling of the age spectrum. Tests of the model show that calculated thermal histories are relatively insensitive to details of parameter selection or the form of the thermal history (Lovera et al. 1991; Harrison et al. 1991*a*; Richter et al. 1991).

The Kailas K-feldspar age spectrum, shown in figure 5*a*, is characterized by ages that rise from 15 to 27 Ma. However, between 20 and 60% gas release, ages average 18.8 ± 0.6 Ma (1$\sigma$ uncertainties), suggesting very rapid cooling at that time. Modeling of this age spectrum provides a more quantitative estimate of this cooling. $^{39}Ar$ diffusivities were calculated (assuming a plane slab geometry) and plotted against the reciprocal heating temperature yielding the Arrhenius plot shown in figure 5*b*. Because of the effects of differing diffusion domain sizes and/or activation energies and the cyclic nature of the laboratory heating schedule (inset to figure 5*b*) needed to bring out the activation parameters, the Arrhenius plot is not an effective way of displaying the domain structure. The diffusion data are shown in figure 5*c* plotted as log $(r/r_0)$ vs. % $^{39}Ar$ released (see Lovera et al., 1991; Harrison et al. 1991*a*). A fit to these data assuming five domains is shown in figure 5*c* and yields good agreement with the empirical results. The two peaks at 20 and 50% $^{39}Ar$ release are an apparent consequence of multiple $E$s together with cycled heating steps (Harrison et al. 1991*a*) and are well duplicated using our choice of parameters (figure 5*c*). The form of the cooling history obtained assuming a single-$E$ for all domains, while offset to lower peak temperatures, is not substan-

tially different to that resulting from the multi-$E$ assumption.

The thermal history was then obtained with the same distribution parameters ($E$ and $D_O/\rho^2$) shown in figure 5*c* by recursively adjusting the input cooling history until the fit to the age spectrum shown in figure 5*d* was achieved. Although imperfect, any further refinements would not materially affect the cooling history. The thermal history (figure 5*d*) is characterized by cooling at a rate of ~5°C/Ma from 27 Ma changing at 19 Ma to a rate of ~100°C/Ma that persisted for at least 2 m.y.

We have analyzed a whole rock split of this sample, which gives the following values: in ppm, Rb = 108.4; Sr = 10.3; $^{87}Rb/^{86}Sr$ = 30.499; $^{87}Sr/^{86}Sr$ = 0.72555(4); Sm = 5.7; Nd = 26.1; $^{147}Sm/^{144}Nd$ = 0.1321; $^{144}Nd/^{143}Nd$ = 0.512616(10); $t_{DM}$ = 1.0 Ga. If we adopt the initial $^{87}Sr/^{86}Sr$ ratio of the Gangdese volcanic suite adjacent Mt. Kailas of 0.70609 (Honnegger et al. 1982) for this sample, we calculate an age of 45 Ma from these data. This age is consistent with an origin of this rock within the Gangdese magmatic belt (e.g., Honegger et al. 1982; Schärer and Allègre 1984): The Sm-Nd depleted model age of 1 Ga is similar to other such data and zircon U-Pb inheritance ages from the Gangdese batholith (e.g., Harris et al. 1988; Xu et al. 1985).

***Bakiya Khola: Paleomagnetism.*** The natural remanent magnetism (NRM) of 101 samples from the Bakiya Khola were measured. Ninety-three of these samples (representing 83 sites) were subjected to thermal demagnetization; seven of these sites have been analyzed in either duplicate or triplicate with no significant difference in the results at a given location. Intensities ranged over three orders of magnitude, reflecting a broad range of lithologic types and magnetic mineral assemblages. Variations in NRM intensity with stratigraphic level are shown in figure 6. The lack of any correlation of magnetic intensity with stratigraphic height strongly suggests that these rocks have experienced essentially no post-depositional remagnetization. A majority of samples showed little change in the direction of magnetization upon heating and were merely reduced in intensity by progressive heating (figure 7). This behavior occurred both in samples that displayed thermally distributed characteristics and those with a more discrete range of blocking temperatures. It is clear that most samples are dominated by a single component of remanence with only minor amounts of other magnetizations. Several of the reversely magnetized samples showed an initial increase in intensity as a minor overprint was removed.

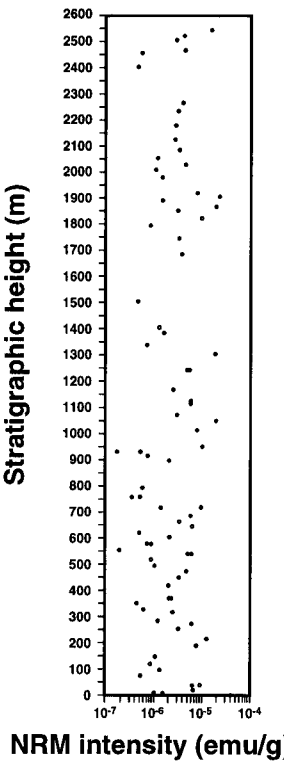


**Figure 6.** Plot of natural remanent magnetism (in emu/g) of 101 samples from the Bakiya Khola against stratigraphic level in the section.

The polarity of stable remanence was easily identified in 74 sites before the 500°C demagnetization step was reached. In the remaining nine samples, however, in spite of further thermal demagnetization through 625°C, the polarity of the stable remanence remained uncertain. Figure 7*c* shows a sample with a stable magnetization intermediate between normal and reverse polarity. Further analysis of sister samples from two such sites have confirmed these intermediate directions; several of the samples displaying intermediate directions lie stratigraphically near a polarity transition, i.e., between clearly normal samples and samples clearly reversely magnetized. The rate of accumulation of the sedimentary material is sufficiently rapid that these directions may reflect variations in the earth's field direction during polarity transitions.

Figure 8 shows our chronostratigraphic interpretation of the paleomagnetic data from Bakiya Khola. While some gaps exist, we feel these preliminary results provide very good constraints on the depositional ages of these rocks. We have chosen to show correlations to both the geomagnetic reversal timescales of Harland et al. (1990) and Cande and

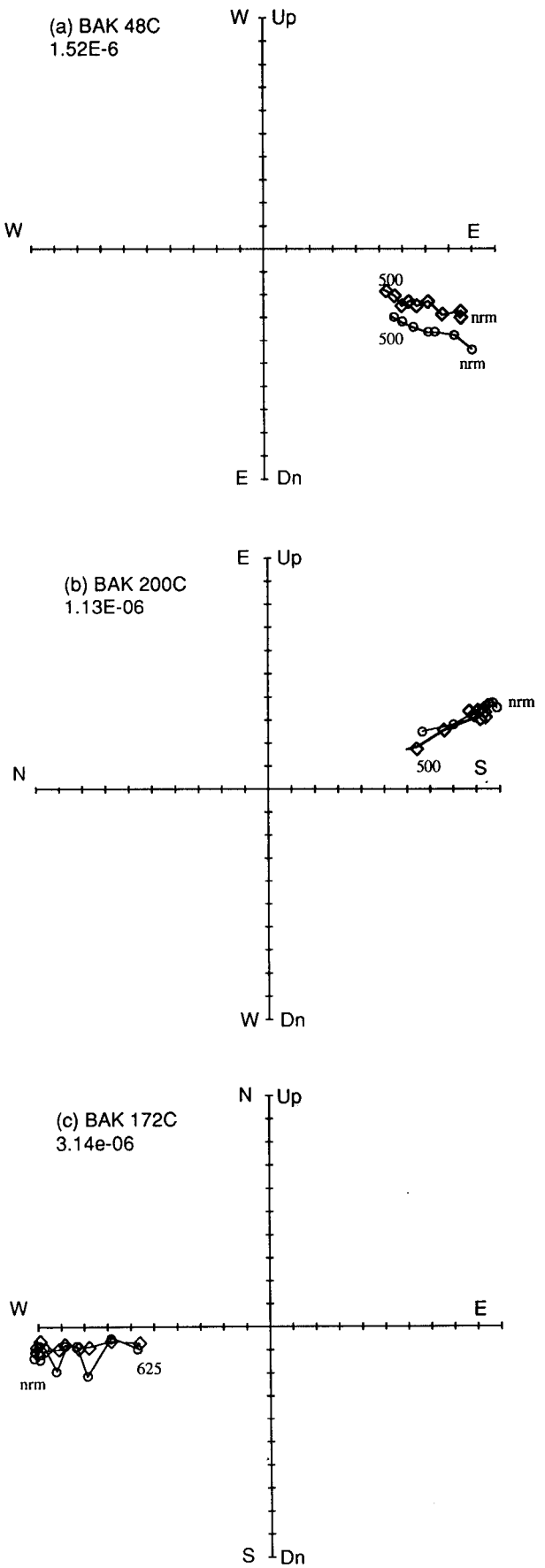


Kent (1992). While each of these timescales have their strengths and weaknesses, there is little significant difference in the interpreted ages from this section using these two chronologies. We began our correlation with the long, dominantly-normal interval at the bottom of our section, which is one of the most prominent features of our polarity section and which we interpret as Anomaly 5. Unfortunately, we have no independent age determinations based on fossil or other chronologic data, but given that this section most likely correlates with the Lower Siwaliks or Middle Siwaliks 1, we feel that the correlations shown in figure 8 are reasonable estimates of the time of deposition for these strata. For subsequent discussion we use the correlation to the timescale of Cande and Kent (1992). For samples above the part of the section sampled for paleomagnetic analysis, we have used the average accumulation rate of 419 m/m.y. to estimate the time of deposition.

***Bakiya Khola: Carbon and Oxygen Isotopes.*** The carbon isotopic composition of buried soil carbonates provides information on the nature of vegetation growing at a site in the course of soil formation (e.g., Cerling 1984; Cerling et al. 1989). Utilization of different metabolic pathways, give rise to three distinct carbon isotopic categories among plants. $C_3$ plants synthesize sugar from three-carbon molecules that tend to favor the lighter isotope, resulting in average $\delta^{13}C_{PDB}$ values of $-27‰$ and includes all trees, most shrubs, and grasses favored by cool growing seasons (Ehleringer 1988). $C_4$ grasses average $-13‰$ in $\delta^{13}C$ and include grasses favored by warm growing seasons. CAM plants, not of importance here, are dominated by succulents and epiphytes. Plants produce large amounts of $CO_2$ as they respire and decay, by far the largest carbon flux in a soil. $\delta^{13}C$ values of soil carbonate forming in equilibrium with the plant carbon reservoir are enriched by 14 to 17‰ over the values in the organic material (Cerling et al. 1989). Thus carbonates formed in the presence of a pure $C_3$ stand will have $\delta^{13}C$ values of $-12$ to $-10‰$, and in the presence of pure $C_4$ plants of around 0 to $+2‰$. In addition, the $\delta^{18}O_{PDB}$ values of soil carbonates can be used to assess the oxygen isotope composition of local rainwater during soil formation.

**Figure 7.** Orthogonal projections for representative samples during heating showing (*a*) normal, (*b*) reversed, and (*c*) ambiguous polarities. Circles = horizontal projections, diamonds = vertical projections. Intensities are in emu/g, temperatures shown by selected steps.

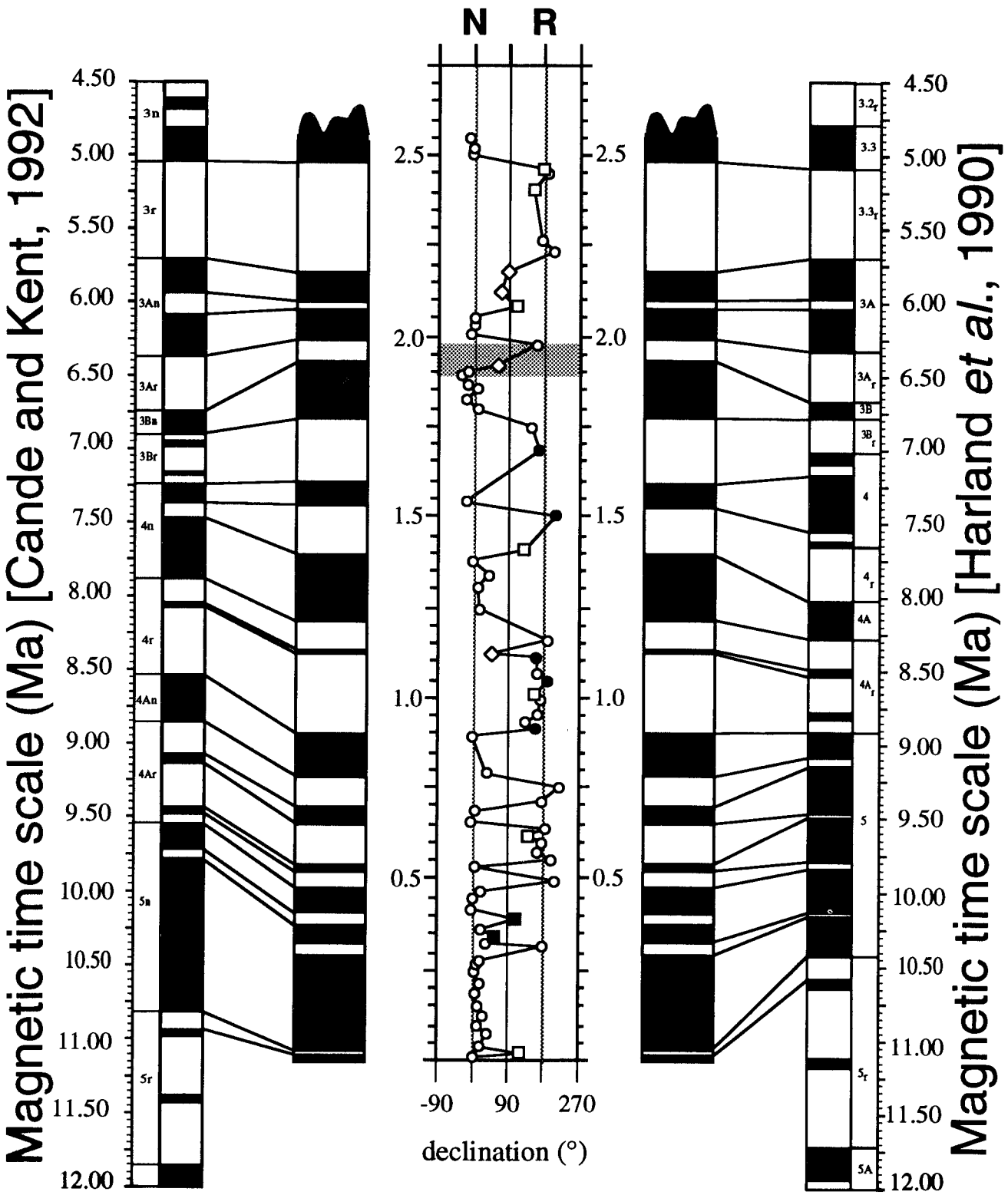


**Figure 8.** Paleomagnetic data and interpretation for Siwalik Group at Bakiya Khola. Center column is the declination of the magnetic vector (with structural correction) after thermal demagnetization at 500°C plotted vs. stratigraphic height (in km). The shaded intervals at ~1.9 km shows the location of the shift in $\delta^{13}C$ values of pedogenic carbonate (see figure 9). Circles are unambiguous results (defined as within 45° of north or south). Ambiguous results (based on both the declination and inclination) are plotted either as squares or diamonds. Diamonds are for ambiguous declinations, converted by 180° so as to plot between 0 and 180° on this diagram. Filled symbols denote the average of samples which have been analyzed in duplicate or triplicate; open symbols represent a single analysis. Identical polarity columns based on these results are compared to the timescales of Harland et al. (1990) and Cande and Kent (1992). The correlation to the scale of Cande and Kent (1992) is used in subsequent diagrams.

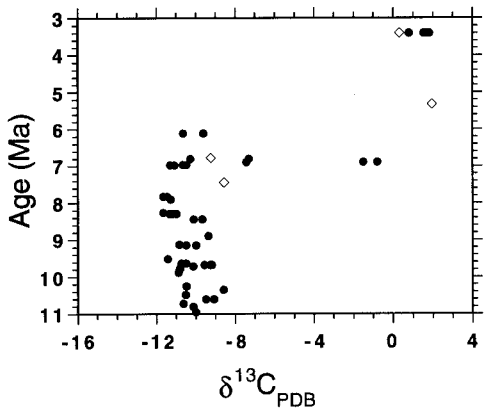


**Figure 9.** Plot of paleosol $\delta^{13}C_{PDB}$ (duplicate analyses included) versus stratigraphic age (correlation to Cande and Kent 1992). Filled circles are carbonate samples; open diamonds are organic samples corrected for the 15‰ fractionation between soil $CO_2$ and the carbonates forming in that soil. Between 10.8 and 7.0 Ma, values average about −10.5‰ but shift at that time to lighter values. This is interpreted to result from a change from a dominantly $C_3$ biomass to $C_4$ as a result of intensification of the Asian Monsoon.

Results of carbon isotopic measurements of both pedogenic carbonate and organic material from Bakiya Khola are shown in figure 9. Between 10.8 and 7.0 Ma, carbonate nodules from the Bakiya section average $-10.5 \pm 0.8$‰ $\delta^{13}C$, whereas organic samples yield values of about −24‰. However, a transition to much lighter values of about −1 to +2‰ occurs at 7.0 Ma. Following from the discussion above, we interpret this shift to result from a change from dominantly $C_3$ plants (i.e., trees) to dominantly $C_4$ (i.e., grasses) plants. Although $C_3$-like values continue to 6.0 Ma and the sample density above the transition decreases markedly, the main significance of these results is the time of first appearance of grasses favored by a warm growing season. The identification of the carbon isotope shift in the Bakiya section further strengthens our interpretation from the magnetic section that the $T_{dep}$ of this section was in the range 11 to 5 Ma.

Quade et al. (1989) first observed this effect in a 18 to 0.4 Ma sequence of Siwalik Group sediments in the Potwar Plateau region of northern Pakistan. The $\delta^{13}C$ values of soil carbonates in that section average about −10‰ between 18 and 7.4 Ma, changing to close to 0‰ between 7.4 and 0.4 Ma. The general agreement between our Bakiya data and this one in the interval of age overlap suggests that there is little if any diachroneity in the arrival of $C_4$ plants throughout the foreland basins of the Himalaya.

For oxygen isotopes, the shift in paleosol $\delta^{18}O_{S\text{-}MOW}$ from relatively light to heavy values at about 7 Ma reported by Quade et al. (1989) is not as clearly evident in our results (table 1). However, the $\delta^{18}O$ values prior to and following the carbon isotope shift at Bakiya Khola of −8.8‰ and −6.6‰, respectively, do suggest a similar effect.

***Bakiya Khola:* $^{40}Ar/^{39}Ar$.** We have analyzed argon isotopes in K-feldspars from coarse sandstones recovered from nine horizons in the Bakiya Khola section following the approach of Copeland and Harrison (1990). We believe that the K-feldspar grains are detritus shed from uplifting basement rocks of the Himalaya and not from an authigenic or volcanic source, because paleotemperatures in these sedimentary rocks are unlikely to have exceeded about 80°C and did not attain temperatures suitable for formation of authigenic K-feldspar, and no magmatism is known to have occurred in the eastern Himalaya during the deposition of this section (see summary in Copeland et al., 1990*a*). Although there appears to be a K-feldspar component eroded from older volcanic rocks in the Pakistani Siwaliks (Harrison et al. 1991*b*), we do not observe concordant age spectra in the Bakiya results characteristic of contemporaneous extrusive rocks.

The concentrates obtained from our density separations contained both sodic and potassic feldspars. However, albitic feldspars commonly yield anomalously old apparent ages due to the presence of extraneous argon. In addition, age uncertainties approaching 100% can arise when backgrounds are large relative to the sample gas. For these reasons we adopted three selection criteria to obtain consistently reliable age data from a single mineral phase. These are: (1) the gas evolved from a crystal contained $>1.5 \times 10^{-15}$ mol $^{39}Ar$ (i.e., greater than about 1% K), (2) had a $^{37}Ar/^{39}Ar < 0.1$ (i.e., a low Ca/K ratio), and (3) the total $^{40}Ar$ was more than three times the product of the mass 36 background and 295.5 (i.e., the proportion of radiogenic $^{40}Ar$ was not significantly influenced by the background correction). Of the 247 grains measured, 117 met these criteria. Of these crystals, 14 yielded ages >500 Ma, but in general they contained $<7 \times 10^{-15}$ mol $^{39}Ar$. Although mica ages are reported from the Lesser Himalayan Formations (LHF) to the northwest of Bakiya that exceed 1400 Ma (Copeland et al. 1991) this Ar concentration corresponds to less than about 2% potassium, leaving open the possibility that these very old dates are in part a reflection of excess Ar.

Minimum ages from each age spectrum or total fusion are plotted in figure 10 as mineral age vs. stratigraphic age, together with a curve showing a

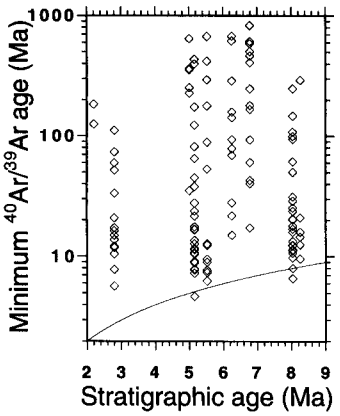


**Figure 10.** Plot of minimum $^{40}Ar/^{39}Ar$ mineral age obtained in low resolution age spectra of detrital K-feldspars from the Bakiya sandstones against stratigraphic age assigned on the basis of our magnetostratigraphy and the magnetic timescale of Cande and Kent (1992) (see figure 8). The curve shown is the 1:1 correspondence between mineral age and age of deposition. That the basement K-feldspar ages approach the stratigraphic age implies very high rates of denudation in the Himalayas.

1:1 correspondence. We take as the minimum age the result that gives the youngest upper age limit at 1σ. Significant features of these results are summarized in table 2.

## Discussion

***Kailas Conglomerate.*** After emplacement, our sample must have been exposed to relatively high temperatures, at least in the range of 400–500°C, for albite blebs to have exsolved on a millimeter scale. Depending on bulk composition, holding anorthoclase at ~550 to 600°C will eventually yield two homogeneous feldspars with compositions of essentially pure albite and $Or_{75}$ (e.g., Yund and Tullis 1983), essentially the observed compositions of our sample. Subsequent slow cooling of the $Or_{75}$ would form perthite with the relative abundances of potassic and sodic phases observed in the thin section (figure 4).

Our proposition is that the protolith was buried to considerable depth by continued surface eruptions that caused an exceedingly thick volcanic pile to accumulate in a relatively short time span. Just how thick this edifice became can be gauged from our estimate of peak temperature, the thermal history derived from the K-feldspar (figure 5*d*), and the character of feldspar unmixing. The length scale of the alkali feldspar exsolution requires the rock to have spent many millions of years at elevated temperatures (Yund 1983). Although very high transient thermal gradients (>100°C/km) could be achieved by contact metamorphism and hydrothermal activity during growth of the volcanic pile, such geotherms could not be sustained in the upper crust for longer than a few million years following cessation of magmatism. The calculated thermal history indicates that the parent rock cooled at about 5°C/Ma between 27 and 19 Ma (figure 5*d*). Such prolonged slow cooling strongly implies a stable crustal thermal structure, which in turn limits the geotherm to a maximum sustainable value of perhaps 40°C/km. Just prior to the onset of rapid cooling at 19 Ma, the sample temperature was >400°C (figure 5*d*) and must have been even higher at an earlier time to permit complete separation of the albite blebs, explain the bulk composition of the microcline, and permit the development of macroperthite. These various arguments suggest that the volcanic (± plutonic) pile must have had a minimum thickness of about 10 km. Because of thermal inertia, the onset of cooling would lag about 1 m.y. behind the onset rapid denudation for a sample originally at ~10 km depth (e.g., Richter et al. 1991).

We conclude that following emplacement close to the earth's surface at ca. 45 Ma, the protolith of our sample was buried to a depth of at least 10 km, where it remained until about 19 Ma when crustal uplift induced rapid denudation (>2 mm/yr). Induced by crustal uplift, the sample once again came close to the surface. It seems reasonable to infer that this event, in which rapid removal of >5 km of presumably volcanic/plutonic overburden occurred, was an important, and perhaps dominant, episode in the formation of the >3 km thickness of the Kailas conglomerate (Heim and Gansser 1939; Gansser 1964). We thus suggest that the Kailas conglomerate (and other correlative deposits adjacent to the Gangdese batholith which contain

**Table 2.** Summary details of $^{40}Ar/^{39}Ar$ dating of detrital K-feldspars, Bakiya Khola

| Sample | # of Grains | Strat. ht. (m) | $t_{DEP}$ (Ma) | $t_{min}$ (Ma) |
|---|---|---|---|---|
| BAK 196 | 2 | 3700 | 2.20 | 125.4 ± 2.0 |
| BAK 195 | 16 | 3450 | 2.80 | 5.7 ± 0.1 |
| BAK 193 | 6 | 2542 | 5.00 | 35.2 ± 0.3 |
| BAK 182 | 27 | 2424 | 5.15 | 7.8 ± 0.3 |
| BAK 176 | 13 | 2244 | 5.53 | 6.3 ± 0.8 |
| PC-91-1 | 17 | 2025 | 6.25 | 15.0 ± 0.4 |
| BAK 158 | 14 | 1927 | 6.78 | 17.3 ± 0.9 |
| BAK 191 | 26 | 1134 | 8.03 | 6.6 ± 1.8 |
| PC-91-2 | 6 | 1055 | 8.25 | 9.9 ± 0.3 |

detritus exclusively from the Gangdese plutonic and volcanic belt) were deposited predominantly during the latest Oligocene or Early Miocene.

This result is of importance for two reasons; age assessment of this unit (Late Eocene to Miocene?) has been problematic (Gansser 1964; Dewey et al. 1988), and Early Miocene unroofing/uplift recognized elsewhere in southern Tibet and the Himalaya has been linked to a major transition in tectonic regime (Harrison et al. 1992*a*). This observation shows that this event was widespread because the Kailas conglomerate extends at least 1000 km along the south margin of the Gangdese batholith between the two localities where we have now detected evidence for this Early Miocene uplift and unroofing.

***Bakiya Khola.*** From the interpretations in figure 8 we may calculate sediment accumulation rates for various time intervals. Using the timescale of Cande and Kent (1992), we have 23 points in our section with known ages of deposition. With these time points we calculated the average accumulation rate for 22 intervals. Figure 11*a* shows accumulation rate versus time with the preferred rates shown by the solid horizontal lines and the range of uncertainty for a given interval with the stippled area. The preferred rate is taken by assigning the stratigraphic thickness of a given polarity interval by placing the boundary midway between points of contrasting polarity. The range of uncertainty is obtained by calculating the rate using the maximum and minimum thicknesses possible given by our data. The solid curve drawn through the stippled boxes is an interpreted curve that yields the same average accumulation rates in essentially every polarity interval (some brief intervals have been ignored). Figure 11*b* is a similar treatment for the correlation to the Harland et al. (1990) timescale. These two interpreted smooth curves are shown together in figure 11*c*.

While there are differences between the two correlations of the Bakiya section (figure 11*c*), certain aspects are common to each. The curves are characterized by marked spikes that increase the rate by up to a factor of 4 within a few thousand years. The average rate of accumulation for the entire section is 0.42 mm/yr and 0.45 mm/yr, based on the Cande and Kent (1992) and Harland et al. (1990) timescales, respectively. However, the range of rates appears to span at least 0.1 to 15 mm/yr, in both cases. The form of the curve is similar in some specific instances, e.g., the peaks at 9.1 Ma and ca. 6.8 Ma.

The basic form of these curves is also seen in the data of Appel et al. (1991) for the Siwaliks of

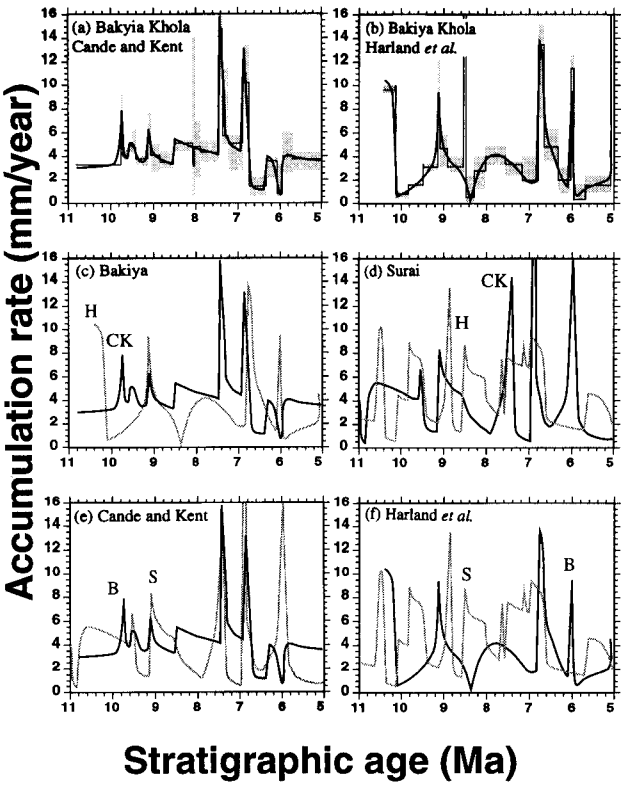


**Figure 11.** Sediment accumulation rate versus age for Siwalik Group sandstones and siltstones, Bakiya Khola and Surai Khola, southern Nepal. (*a*) Data for Bakiya Khola showing uncertainties based on the correlation (figure 8) to the magnetic timescale of Cande and Kent (1992). Shaded region indicates the range of uncertainty for average accumulation rate and for individual polarity chron. Solid horizontal lines are average rates calculated assuming thickness of interval is defined by the midpoint between samples that define the polarity transition. Solid curved line is interpreted history that gives the same averages as the horizontal lines. (*b*) Same as in (*a*) but using the correlation (figure 8) to the timescale of Harland et al. (1990). (*c*) Comparison between the Harland et al. (1990) [H] and Cande and Kent (1992) [CK] timescales for Bakiya Khola. (*d*) Comparison between the Harland et al. (1990) [H] and Cande and Kent (1992) [CK] timescales for interpretation of the data of Appel et al. (1991) for Surai Khola. (*e*) Comparison between the sediment accumulation histories at Bakiya Khola (B) and Surai Khola (S) based on the timescale of Cande and Kent (1992). (*f*) Comparison between the sediment accumulation histories at Bakiya Khola (B) and Surai Khola (S) based on the timescale of Harland et al. (1990).

Surai Khola, approximately 250 km to the west (figure 11*d*). Again, the choice of timescale effects the details of the curve but the over-all character of these curves is substantial and rapid variability. Certain features are also quite robust, appearing regardless of the timescale used (e.g., the spike at

ca. 9.5 Ma and the rapid increase from ~2mm/yr to ~8.5 mm/yr followed by a more gentle decline over ~800,000 years that begins at 9.2 Ma on the Cande and Kent [1992] correlation and is shifted to 8.6 Ma on the Harland et al. [1990] correlation).

These curves are consistent with the tectonics of the region and show variability consistent with the timescale and magnitude of tectonic activity. The tectonics of the source area of the Siwaliks is dominated by shortening via thrusting and folding. Thrusting in a highland will locally produce greater relief and consequently increase the rate of erosion and transport of material to the foreland basin. As erosion removes material from the uplifted terrain, the rate of removal decreases. The sediment accumulation curves at Bakiya Khola and Surai Khola are consistent with a repetition of several of these events and suggest the timescale and magnitude of tectonic activity.

An alternate explanation might be that the observed variations (figure 11) correspond only to rates of sediment supply to this portion of the basin and not changes in denudation rate in the source. The major river return period estimated in the Pakistani Siwaliks is only between 10,000 and 100,000 yrs (Johnson et al. 1985), whereas the period of the observed accumulation rate variations in the Bakiya section is 500,000 to 1 m.y. Indeed, Holmes (1965) has documented the evulsion of the Sapt Kosi River in southeastern Nepal over 60 km in the interval 1736 to 1949. Moreover, the eastern Nepal Siwaliks are not characterized by the channel and overbank deposits of meandering river systems common in Pakistan (Badgley and Behrensmeyer 1980). Rather they appear to have been deposited in poorly drained areas (West et al. 1991) that would be less likely to experience periodic fluctuations in sediment supply. Thus we must call on another effect to explain our data.

The sediment-accumulation curves from Bakiya Khola and Surai Khola are compared in figure 11*e* and 11*f*. Using the timescale of Cande and Kent (1992), the two curves share several similarities (figure 11*e*). The period from 11 to 8 Ma is less variable that the interval from 8 to 5 Ma in both curves and three peaks are matched quite well (9.1 to 8.5 Ma, 7.4 Ma, and 6.8 Ma). However, the timescale of Harland et al. (1990) shows much less similarity between these two sites (figure 11*f*). It is difficult to say if one timescale is clearly superior to other published magnetic timescales (the data used are different) so we cannot definitively conclude whether the sediment-accumulation history at these two sites was grossly similar (i.e., accumulation rates in the Late Miocene both about 0.4 mm/yr) or much more so with inflections and magnitudes matched many times during a 6 m.y. period. More sections need to be documented to determine if comparisons of Siwalik sections so far apart are warranted.

If we consider tectonics the prime influence on sedimentation in the Siwalik basin, the similarity between these two sites suggests very similar tectonic activity over a 250 or more km segment of the orogen for at least 3.5 m.y. Episodic movement on the Main Boundary Thrust, a steeply N-dipping late Neogene fault that marks the contact between the Lesser Himalayan Formations (LHF) and the Siwaliks (or cold thrusts within the LHF) (Gansser 1964; Molnar 1984; Le Fort 1975; Pêcher and Le Fort 1986), could have produced significant Late Miocene topographic excursions leading to the observed sediment accumulation. For example, integrated motion over 0.5 to 1 m.y. at slip rates of 10–20 mm/yr (Lyon-Caen and Molnar 1985; Molnar 1987; Armijo et al. 1986) on 30° crustal-scale thrust faults could easily produce km-scale relief in a zone many kilometers wide.

Sandstone samples from nine horizons of ~2.2 to 8.25 Ma yield $^{40}Ar/^{39}Ar$ minimum ages ($n$ = 117) that range from essentially indistinguishable from the stratigraphic age to >1000 m.y. older (figure 10) but generally cluster within ~15 m.y. of the depositional age. This is surprising because the very low resolution of the age spectra tends to conceal the true minimum age. Thus, the average age difference of 3.5 m.y. is still an upper limit to the duration between argon closure and deposition. The generally close correspondence between the youngest mineral age and stratigraphic age is remarkable because the K-feldspar must travel from a substantial depth (corresponding to the $T_C$ of 150–200°C) to the surface to be eroded and transported to the deposition site within a few million years. For the geothermal structure expected during thrusting, this average age difference implies that at least a portion of the source region was unroofing at a minimum rate of 2 mm/yr. Clearly in some instances the unroofing rate was substantially higher (e.g., BAK 176).

We have argued (Copeland et al. 1991; Copeland and Harrison 1990) that very young mineral ages shed from the Himalaya between 5 and 3 Ma may have begun to acquire their radiogenic argon at relatively shallow depths due to a hydrothermal system then active in the Main Central Thrust zone. However, we are not aware of any evidence suggesting that a similar system was extant in this region between 9 and 6 Ma and thus concur with the conclusion of Copeland and Harrison (1990)

that exceedingly high rates of denudation were occurring in places in the Himalaya during the Mid- to Late Miocene. Even if such a hydrothermal system existed at an earlier time (with a geothermal gradient as high as 100°C/km), minimum denudation rates of >2 mm/yr would still be implied for some samples.

Another characteristic of the $^{40}Ar/^{39}Ar$ data is the pronounced clustering of minimum ages between 21 and 7 Ma. About half (59 out of 117) of all grains from the Bakiya section yield minimum ages in this range, compared to only 11 grains that yield minimum ages between the first contact of India with Asia (~50 Ma) and 25 Ma. Thus, the rocks shedding detritus into the foreland basin were generally not characterized by cooling histories suggestive of rapid unroofing during the Paleogene. Harrison et al. (1992*a*) called attention to a widespread transition from low to very high denudation rates throughout the Himalaya and southern Tibet beginning in the Early Miocene. They ascribed this coincidence to the termination of left-lateral strike-slip motion on the Red River fault zone at that time (Tapponnier et al. 1986; Harrison et al. 1992*b*). Thereafter, the Main Central Thrust (Brunel 1975; Hodges et al. 1988; Hubbard and Harrison 1989; Copeland et al. 1990*a*) and Gangdese Thrust (Yin et al. 1992) probably accommodated much of the continued northward convergence of India, resulting in rapid uplift of the Tethyan Himalaya and Gangdese belt. Thus, the Himalaya and southern Tibet did not experience significant crustal thickening and consequent uplift/unroofing until the Early Miocene; rapid unroofing rates have been a feature of some portions of the Himalaya since then. The results presented in this paper, both from Kailas and the Bakiya Khola, support that view.

Our observation of a carbon isotope shift in eastern Nepal at 7 Ma (figure 9) confirms the view of Quade et al. (1989) that the shift from $C_3$ to $C_4$ plants at that time was a widespread phenomenon. Those authors principally ascribed this transition to an intensification of the Asian Monsoon (Ruddiman and Kutzbach 1989) causing seasonal fluctuations in rainfall that tended to favor grasses over trees. However, they also acknowledged that the Late Miocene marks the first global appearance of many $C_4$ plants (perhaps due to reduced atmospheric $CO_2$ levels) and that the isotope shift might also be due to successful competition even without a changing climate. However, several independent lines of evidence tend to support a climate change at that time. Although not as distinctive as carbon, oxygen isotopes also show a shift to heavier compositions at about 8–7 Ma (Quade et al. 1989). Because this effect reflects local changes to the rainfall rather than plant activity, they concluded that a change in climate occurred at that time. This shift is less clear, but still consistent with the oxygen isotopic compositions of Late Miocene paleosols in the Bakiya Khola. Increases in opal accumulation and deposition of marine organic carbon, the appearance of fauna characteristic of cold water and high nutrient content in the Arabian Sea, and changes of fossil rodent taxa in the Pakistani Siwaliks, all occurring at about 8–7 Ma, suggest intensification of the Asian monsoon (Murray and Prell 1991; Prell and Kutzbach 1991; Meyers 1991; Kroon et al. 1991; Jacobs and Flynn 1981).

The intensity of the Asian monsoon is owed to the extraordinarily elevated Tibetan plateau. During summer months, solar energy is efficiently transferred to the atmosphere above the plateau. As this warm air rises, it spreads laterally, creating a low-pressure area that draws in moist air from the Indian Ocean resulting in highly seasonal precipitation. Results of atmospheric circulation modeling (Ruddiman and Kutzbach 1989, 1991) suggest that uplift of the Tibetan plateau to something near its present elevation and size would be required to initiate this effect. We concur with Quade et al. (1989) that the fundamental cause for the carbon isotope shift in pedogenic carbonates is tectonic in origin, i.e., the uplift of the Tibetan plateau.

## Conclusions

In this paper we have described two contrasting applications of isotopic techniques in a molasse basin setting; one in which the basement thermal history preserved in a conglomerate clast permits estimation of its poorly known depositional age, and one in which independent determination of the chronostratigraphy allows a more detailed understanding of the rates of unroofing and uplift of the source area. Paleomagnetic measurements of a section of Siwalik Group sandstones and siltstones in Bakiya Khola, southeastern Nepal, reveal depositional ages of between 10.8 and 4.9 Ma. Younger strata in this section are estimated to have been deposited as recently as 2.2 Ma. Sediment accumulation rates are high and vary in a cyclic fashion between 0.1 and 15 mm/yr with a period of between 400,000 yrs and 1 m.y. that may reflect episodic thrusting in the Himalaya. $^{40}Ar/^{39}Ar$ dating of single detrital K-feldspars from nine Bakiya Khola horizons with depositional ages of ~2.2 to 8.25 Ma yield minimum ages typically within 3

m.y. of their deposition age, indicating exceptionally rapid unroofing in the Himalaya throughout that interval. Half the grains from all analyzed horizons in the Bakiya section yield minimum ages between 5 and 25 Ma. This latter age corresponds to the onset of a widespread unroofing event throughout the Himalaya and southern Tibet, and data from Nepal suggest the time between the change in Pakistan and Nepal was no more than about 1 m.y.

Pedogenic carbonates from Bakiya Khola yield $\delta^{13}C$ values of $-10.5‰$ between 11 and 7 Ma, changing after that time to much heavier values. This shift, previously recognized in Siwalik Group sediments in Pakistan, suggests change from dominantly $C_3$ to dominantly $C_4$ plants. This significant ecological shift is likely related to intensification of the Asian Monsoon brought about by uplift of the Tibetan Plateau.

In south-central Tibet, the Kailas conglomerate developed a thickness of over 3 km due to uplift and erosion of the Gangdese belt. $^{40}Ar/^{39}Ar$ K-feldspar results from a cobble out of this conglomerate originally derived from Gangdese volcanic rocks yields an age spectrum characterized by relatively slow cooling (5°C/Ma) between 27–19 Ma followed by very rapid cooling (100°C/Ma) between 19–18 Ma. Although the rock retains volcanic features, the feldspar microstructure indicates that it has been heated to >400°C subsequent to eruption at ca. 45 Ma. This thermal history is consistent with deep burial in the volcanic pile followed by rapid unroofing beginning at 20 to 19 Ma. The Early Miocene rapid unroofing event recorded by the sample is the same age as that recognized in the Gangdese belt 1000 km farther east, near Lhasa; the results reported here suggest that this event was regionally important. The unroofing event of, and the derivation of the thick Kailas conglomerate from the Gangdese belt is a consequence of movement on the Gangdese thrust system (Yin et al. 1992). These results suggest an Early Miocene upper limit of the depositional age of the Kailas conglomerate significantly younger than most previous estimates.

## ACKNOWLEDGMENTS

We thank Ing. Fritz Moravec for collecting the Kailas cobble and Ms. Sophie Kidd for helping us acquire it. We thank Marty Grove for electron microprobe measurements, Matt Heizler, Peter Holden, Chen Wenji, Dave Winter, and Linda Civil (ANU) for isotope analyses, Bill Akers for Macspertise, Gary Cook for expiditing the neutron irradiations, and Oscar Lovera for assistance with the modeling. We thank Doug Burbank, Peter Zeitler, and Terry Jordan for helpful reviews, and Bob Newton and Fred Anderson for their invitation to present this paper at the Centennial Symposium and their supportive comments. This research was funded from grants from the UCLA Senate, the Australian National University, University of Houston, NSF, and the DoE Office of Basic Energy Sciences.

## REFERENCES CITED

Appel, E.; Rosler, W.; and Corvinus, G., 1991, Magnetostratigraphy of the Miocene-Pleistocene Surai Khola Siwaliks in West Nepal: Geophys. Jour. Int., v. 105, p. 191–198.

Armijo, R. P.; Tapponnier, P.; Mercier, J. L.; and Han, T. L., 1986, Quaternary extension in southern Tibet: field observations and tectonic implications: Jour. Geophys. Res., v. 91, p. 13,803–13,872.

Badgley, C., and Behrensmeyer, A. K., 1980, Paleoecology and middle Siwalik sediments and faunas, northern Pakistan: Paleogeog. Paleoclimat. Paleoecol., v. 30, p. 133–155.

Baur, H., 1980, Numersche simulation und praktishe Erprobung einer rotationssymmetrischen lonenquelle für Gasmassenspektrometer: Unpub doctorate thesis, ETH, Zurich.

Beaubouef, R.; Casey, J. F.; Hall, S. A.; and Evans, I. A., 1990, A paleomagnetic investigation of the Lower Ordovician St. George Group, Port-au-Port Peninsula, Newfoundland: implications for the Iapetus Ocean and evidence for Late Paleozoic remagnitization: Tectonophysics, v. 182, p. 337–356.

Brunel, M., 1975, La nappe du Mahabharat, Himalaya du Nepal Centrale: C. R. Seances Acad. Sci., v. 280, p. 551–554.

Cande, X.; and Kent, C., 1992, A new geomagnetic polarity time scale for the Late Cretaceous and Cenozoic: Jour. Geophys. Res., v. 97, p. 13,917–13,952.

Cerling, T. E., 1984, The stable isotopic composition of modern soil carbonate and its relationship to climate: Earth. Planet. Sci. Letters, v. 71, p. 229–240.

———; Quade, J.; Wang, Y.; and Bowman, J. R., 1989, Carbon isotopes in soils and paleosols as ecology and paleoecology indicators: Nature, v. 341, p. 138–139.

Cerveny, P. F.; Naeser, N. D.; Zeitler, P. K.; Naeser, C. W.; and Johnson, N. M., 1988, History of uplift and relief of the Himalaya during the past 18 Ma: evidence from fission-track ages of detrital zircon from sand-

stones of the Siwalik Group; *in* Kleinspehn, K. L., and Paola, C., eds., New Perspectives in Basin Analysis, New York, Springer-Verlag, p. 43–61.

Cochran, J. R., 1990, Himalayan uplift, sea level, and the record of Bengal Fan sedimentation: Proc. Ocean Drill. Prog. Sci. Results, v. 116, p. 397–416.

Copeland, P., and Harrison, T. M., 1990, Episodic rapid uplift in the Himalaya revealed by $^{40}Ar/^{39}Ar$ analysis of detrital K-feldspar and muscovite, Bengal Fan: Geology, v. 18, p. 354–357.

———; ———; and Heizler, M. T., 1990*b*, $^{40}Ar/^{39}Ar$ single-crystal dating of detrital muscovite and K-feldspar from ODP Leg 116, southern Bengal Fan: implications for the uplift and erosion of the Himalaya: Proc. Oceanic Drilling Prog. Sci. Results, v. 116, p. 93–114.

———; ———; Hodges, K. V.; Maruéjol, P.; Le Fort, P.; and Pêcher, A., 1991, An early Pliocene thermal disturbance of the Main Central Thrust, central Nepal: implications for Himalayan tectonics: Jour. Geophys. Res., v. 96, p. 8475–8500.

———; ———; Kidd, W. S. F.; Ronghua, X.; and Yuquan, Z., 1987, Rapid Early Miocene acceleration of uplift in the Gangdese Belt, Xizang-southern Tibet, and its bearing on accommodation mechanisms of the India-Asia collision: Earth Planet. Sci. Letters, v. 86, p. 240–252.

———; ———; and Le Fort, P., 1990*a*, Age and cooling history of the Manaslu granite: implications for Himalayan tectonics: Jour. Vol. Geotherm. Res., v. 44, p. 33–50.

Corvinus, G., 1988, The mio-plio-pleistocene litho- and biostratigraphy of the Surai Khola Siwaliks in West-Nepal: first results: C. R. Acad. Sci. Paris, v. 306, p. 1471–1477.

DePaolo, D. J., 1981, Neodymium isotopes in the Colorado Front Range and crust-mantle evolution in the Proterozoic: Nature, v. 291, p. 193–196.

Dewey, J. F., and Burke, K. A., 1973, Tibetan, Variscan, and Precambrian basement reactivation: products of continental collision: Jour. Geology, v. 81, p. 683–692.

———; Shackelton, R. M.; Chengfa, C.; and Yiyin, S., 1988, The tectonic evolution of the Tibetan Plateau: Royal Soc. (London) Philos. Trans.: v. A327, p. 379–413.

Dickinson, W. R., 1974, Plate tectonics and sedimentation, *in* Tectonics and Sedimentation: Soc. Econ. Paleont. Mineral. Spec. Paper 22, p. 1–27.

Dodson, M. H., 1973, Closure temperature in cooling geochronological and petrological systems: Contrib. Mineral. Petrol., v. 40, p. 259–274.

Ehleringer, J. R., 1989, Carbon isotope ratios and physiological processes in arid zone plants *in* Rundel, J. W., ed., Applications of Stable Isotope Ratios to Ecological Research: New York, Springer-Verlag, p. 41–54.

Froude, D. O.; Ireland, T. R. et al., 1983, Ion microprobe identification of 4100–4200 Myr-old terrestrial zircons: Nature, v. 304, p. 616– 618.

Gansser, A., 1964, The Geology of the Himalayas, New York, Wiley Interscience, 289 p.

Gartner, S., 1990, Neogene calcareous nanofossil biostratigraphy, Leg 116 (Central Indian Ocean): Proc. Ocean Drill. Prog. Sci. Results, v. 116, p. 165–187.

Harland, W. B.; Armstrong, R. L.; Cox, A. V.; Craig, L. E.; Smith, A. G.; and Smith, P. G., 1990, A Geologic Timescale 1989 (2d ed.): New York, Cambridge University Press, 263 p.

Harris, N. B. W.; Xu Ronghua; Lewis, C. L.; Hawkesworth, C. J.; and Zhang Yuquan, 1988, Isotope geochemistry of the 1985 Tibet Geotraverse, Lhasa to Golmud, Royal Soc. (London) Philos. Trans.: v. A327, p. 263–285.

Harrison, T. M.; Copeland, P.; Burner, S.; Zeitler, P.; Quade, J.; Kidd, W. S. F.; and Ojha, T. P., 1991*b*, Detrital ages of Himalayan (Siwalik) and Tibetan (Kailas) Molasse: EOS, v. 72, p. 251.

———, ———, Kidd, W. S. F.; and Yin, A., 1992*a*, Raising Tibet: Science, v. 255, p. 1663–1670.

———; Lovera, O. M.; and Heizler, M. T., 1991*a*, $^{40}Ar/^{39}Ar$ results for alkali feldspars containing diffusion domains with differing activation energy: Geochim. Cosmochim. Acta, v. 55, p. 1435–1448.

———; Wenji, C.; LeLoup, P. H.; Ryerson, F. J.; and Tapponnier, P., 1992*b*, An Early Miocene transition in deformation regime within the Red River fault zone, Yunnan, and its significance for Indo-Asian tectonics: *Jour. Geophys. Res.*, v. 97, p. 7159–7182.

Heim, A., and Gansser, A., 1939, Central Himalaya, geological observations of the Swiss expedition 1936: Mem. Soc. Helv. Nat., v. 73, p. 1–245.

Hodges, K. V.; Hubbard, M. S.; and Silverberg, D.; 1988, Metamorphic constraints on the thermal evolution of the central Himalayan orogen: Royal Soc. (London) Philos. Trans.: v. A326, p. 257–286.

Holmes, A., 1965, Principles of Physical Geology: London, Thomas Nelson and Sons, 1288 p.

Honegger, K.; Deitrich, V.; Frank, W.; Gansser, A.; Thoni, M.; and Trommsdorff, V., 1982, Magmatism and metamorphism in the Ladakh Himalayas (the Indus-Tsangpo suture zone): *Earth Planet. Sci. Letters*, v. 60, p. 253–292.

Hubbard, M. S., and Harrison, T. M., 1989, $^{40}Ar/^{39}Ar$ age constraints on deformation and metamorphism in the MCT Zone and Tibetan Slab, eastern Nepal Himalaya: Tectonics, v. 8, p. 865–880.

Ingersoll, R. V., 1988, Tectonics of sedimentary basins: Geol. Soc. America Bull., v. 100, p. 1704–1719.

Jacobs, L. L., and Flynn, L. J., 1981, Development of the modern rodent fauna of the Potwar Plateau, northern Pakistan: Proc. Neogene/Quaternary Boundary Conf., India, 1979, p. 79–82.

Johnson, N. M.; Opdyke, N. D.; Johnson, G. D.; Lindsay, E. H.; and Tahirkheli, R. A. K., 1982, Magnetic polarity stratigraphy and ages of the Siwalik Group rocks of the Potwar Plateau, Pakistan: Paleo. Paleo. Paleo., v. 37, p. 17–42.

———; Stix, J.; Tauxe, L.; Cerveny, P. F.; and Tahirkheli, R. A. K., 1985, Paleomagnetic chronology, fluvial processes, and tectonic implications of the Siwalik deposits near Chinji village, Pakistan: Jour. Geology, v. 93, p. 27–40.

Kroon, D.; Steens, T.; and Troelstra, S. R., 1991, Onset of monsoonal related upwellings in the western Arabian Sea as revealed by planktonic foraminifers: Proc. Ocean Drill. Prog. Sci. Results, v. 117, p. 257–263.

Le Fort, P., 1975, Himalaya, the collided range: present knowledge of the continental arc: Am. Jour. Sci., v. 275A, p. 1–44.

Lovera, O. M.; Richter, F. M.; and Harrison, T. M., 1989, $^{40}Ar/^{39}Ar$ geothermometry for slowly cooled samples having a distribution of diffusion domain sizes: Jour. Geophys. Res., v. 94, p. 17,917–17,935.

Lovera, O. M.; Heizler, M. T.; and Harrison, T. M., 1992, Argon diffusion domains in K-feldspar II: kinetic properties of MH-10: Contrib. Mineral. Petrol., in press.

———; Richter, F. M.; and Harrison, T. M., 1991, Diffusion domains determined by $^{39}Ar$ release during step-heating: Jour. Geophys. Res., v. 96, p. 2057–2069.

Lyon-Caen, H., and Molnar, P., 1985, Gravity anomalies, flexure of the Indian plate, and the structure, support, and evolution of the Himalaya and Ganga basin: Tectonics, v. 4, p. 513–538.

McCrea, J. M., 1950, On the isotopic chemistry of carbonates and a paleotemperature scale: Jour. Chem. Phys., v. 18, p. 849–857.

McDougall, I., and Harrison, T. M., 1988, Geochronology and Thermochronology by the $^{40}Ar/^{39}Ar$ Method: New York, Oxford University Press, 212 p.

Meyers, P. A., 1991, Enhanced burial of organic carbon in Indian Ocean sediments as a result of the Himalayan and Tibetan plateau uplift: EOS, v. 72, p. 258.

Miller, D. S.; Duddy, I. R.; Green, P. F.; Hurford, A. J.; and Naeser, C. W., 1985, Results of interlaboratory comparison of fission-track age standards: Fission-Track Workshop-1984: Nucl. Tracks, v. 10, p. 383–391.

Molnar, P., 1984, Structure and tectonics of the Himalaya: constraints and implications of geophysical data: Ann. Rev. Earth Planet. Sci., v. 12, p. 489–518.

———, 1987, Inversion of profiles of uplift rates for the geometry of dip-slip faults at depth, with examples from the Alps and the Himalaya: Ann. Geophys., v. 5B, p. 663–670.

Murray, D., and Prell, W., 1991, Faunal evidence for increased Monsoon circulation in the Arabian Sea near 8 Ma.: EOS, v. 72, p. 258.

Nelson, S. T., and Davidson, J. P., 1992, Interactions between mantle-derived magmas and mafic crust, Henry Mountains, Utah: Jour. Geophys. Res., in press.

Pêcher, A., and Le Fort, P., 1986, The metamorphism in central Himalaya, its relations with the thrust tectonic: Science de la Terre Mém. 47, p. 285–309.

Prell, W. P., and Kutzbach, J. E., 1991, Sensitivity of the Indian Monsoon to changes in tectonic (orographic), orbital (solar radiation), and glacial boundary conditions: model-data comparison: EOS, v. 72, p. 257–258.

Quade, J.; Cerling, T. E.; and Bowman, J. R., 1989, Dramatic ecologic shift in the latest Miocene of northern Pakistan, and its significance to the development of the Asian Monsoon: Nature, v. 342, p. 163–166.

Richter, F. M.; Lovera, O. M.; Harrison, T. M.; and Copeland, P., 1991, Tibetan tectonics from $^{40}Ar/^{39}Ar$ analysis of a single K-feldspar sample: Earth Planet. Sci. Letters, v. 105, p. 266–278.

Ruddiman, W. F., and Kutzbach, J. E. 1989, Forcing of Late Cenozoic northern hemisphere climate by plateau uplift in southern Asia and the American West: Jour. Geophys. Res., v. 94, p. 18,409–18,427.

———, and ———, 1991, Plateau uplift and climatic change: Sci. American, vol. 246, p. 66–75.

Schärer, U., and Allègre, C. J., 1984, U-Pb geochronology of the Gangdese (Transhimalaya) plutonism in the Lhasa-Xigaze region, Tibet: Earth Planet. Sci. Letters, v. 63, p. 423–432.

Tapponnier, P.; Peltzer, G.; and Armijo, R., 1986, On the mechanics of the collision between India and Asia, *in* Coward, M. P., and Ries, A. C., eds., Collision tectonics: Geol. Soc. Spec. Pub. 19 p. 115–157.

West, R. M.; Hutchison, J. H.; and Munthe, J., 1991, Miocene vertebrates from the Siwalik Group, western Nepal: Jour. Vert. Paleo., v. 11, p. 108–129.

Yin, A.; Harrison, T. M.; Ryerson, F. J.; Kidd, W. S. F.; Copeland, P.; and Chen Wenji, 1992, The Gangdese Thrust revealed: EOS, v. 73, p. 545.

Yund, R. A., 1983, Diffusion in feldspars, *in* Ribbe, P. H., ed., Feldspar Mineralogy (Mineral. Soc. America Reviews in Mineralogy Vol. 2): p. 203–222.

Yund, R. A., and Tullis, J., 1983, Subsolidus phase relations in the alkali feldspars with emphasis on coherent phases, *in* Vol. 2, Ribbe, P. H., ed., Feldspar Mineralogy, (Mineral. Soc. America Reviews in Mineralogy Vol. 2): p. 141–176.